

Title	Intrinsic proton conduction in 2D sulfonated covalent organic framework through the post-synthetic strategy
Author(s)	Zhang, Yuwei; Li, Chunzhi; Liu, Zhaohan; Yao, Yuze; Hasan, Md. Mahmudul; Liu, Qianyu; Wan, Jieqiong; Li, Zhongping; Li, He; Nagao, Yuki
Citation	CrystEngComm, 23: 6234-6238
Issue Date	2021-08-13
Type	Journal Article
Text version	author
URL	http://hdl.handle.net/10119/18026
Rights	Copyright (C) 2021 Royal Society of Chemistry. Yuwei Zhang, Chunzhi Li, Zhaohan Liu, Yuze Yao, Md. Mahmudul Hasan, Qianyu Liu, Jieqiong Wan, Zhongping Li, He Li and Yuki Nagao, CrystEngComm, 23, 2021, 6234-6238. https://doi.org/10.1039/D1CE00957E
Description	

COMMUNICATION

Intrinsic proton conduction in 2D sulfonated covalent organic framework through the post-synthetic strategy

Received 00th January 20xx,
Accepted 00th January 20xx

Yuwei Zhang,^{a†} Chunzhi Li,^{b†} Zhaohan Liu,^c Yuze Yao,^c Md. Mahmudul Hasan,^c Qianyu Liu,^a Jieqiong Wan,^d Zhongping Li,^{c*} He Li^{b*} and Yuki Nagao^{c*}

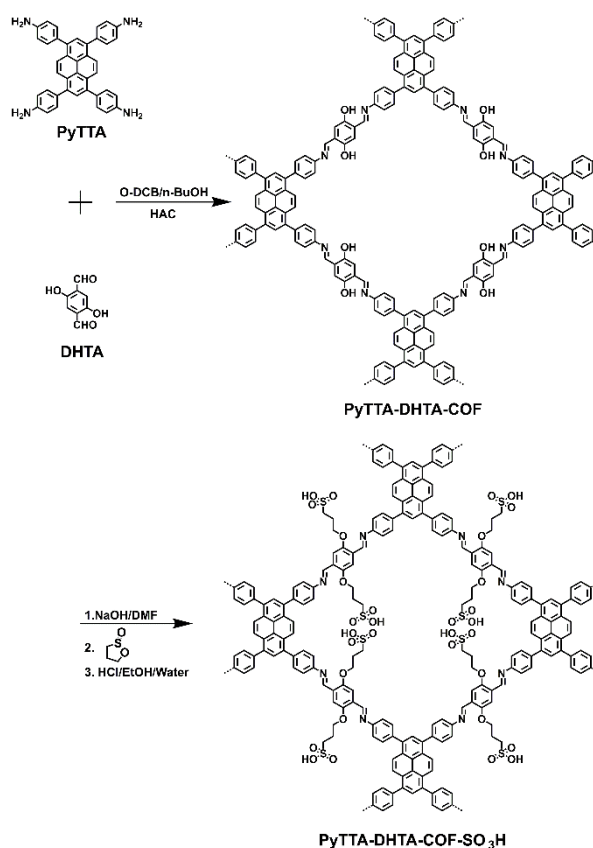
DOI: 10.1039/x0xx00000x

Two-dimensional covalent organic frameworks (2D COFs) have attracted much attentions in proton conduction, owing to their regular pore channels and easy functionalization. However, most of COFs required the loading of proton carriers to achieve high proton conductivity. Here, we report the immobilization of flexible sulfonic acid groups on the channel walls of PyTTA-DHTA-COF (synthesized by condensation of 4,4',4'',4'''-(pyrene-1,3,6,8-tetrayl)tetraaniline and 2,5-dihydroxyterephthalaldehyde) via a simple post-synthetic modification strategy. The sulfonated COF showed intrinsic proton conductivity up to 10^{-3} at 25 °C and 100% relative humidity (RH), and high conductivity up to 10^{-2} S cm⁻¹ under at 70 °C and 100% RH without introduction of any non-covalent acid molecules or imidazole derivatives.

There is a widely accepted realization that energy consumption has been a serious problem for the development of modern civilization during the last past decades. In the face of detrimental effects, effective technologies and new materials are urgent and essential to exploitation. The last past has witnessed the rapid development of proton-exchange membrane fuel cells that serve as a typical representative of clean energy.¹ Nafion is a typical commercial high-proton conductive membrane. However, high cost and contamination are very serious owing to the fluorohydrocarbon structure. Therefore, the design of alternative functional materials to fabricate proton exchange membrane is of high importance.²⁻³

Porous materials, such as inorganic zeolite, metal-organic frameworks (MOFs), porous organic polymers (POPs) and

covalent organic frameworks (COFs) with high porosity have been extensively investigated for proton conductivity.³⁻⁵



Scheme 1. Design and synthesis of PyTTA-DHTA-COF and PyTTA-DHTA-COF-SO₃H.

Comparing to other traditional porous materials, two-dimensional COFs possess intriguing aesthetic architectures, high porosity, good thermal and chemical stability.⁶⁻¹⁰ Especially, owing to the periodic columnar π -arrays and uniform 1D nanopores, 2D COFs have shown potential applications in ions and proton conductivity.¹¹⁻¹⁷ The pre-designed 2D COF made it much easier for the proton-containing carriers to be doped or

^a Laboratory of Preparation and Applications of Environmental Friendly Materials (Jilin Normal University), Ministry of Education, Changchun, 130103, China.

^b State Key Laboratory of Catalysis, Dalian Institute of Chemical Physics, Chinese Academy of Sciences, Dalian, 116023, China. E-mail: lihe@dicp.ac.cn (H. Li).

^c School of Materials Science, Japan Advanced Institute of Science and Technology, Ishikawa 923-1211, Japan. E-mail: lizhongping2021@yonsei.ac.kr (Z. Li); ynagao@jaist.ac.jp (Y. Nagao).

^d College of Chemistry and Chemical Engineering, Shanghai University of Engineering Science, Shanghai, 201620, China.

† These authors contributed equally.

Electronic Supplementary Information (ESI) available: [details of any supplementary information available should be included here]. See DOI: 10.1039/x0xx00000x.

anchored. For example, 2D imine-linked TPB-DMTP-COF with high porosity loaded plentiful triazoles to achieve high proton conductivity of $1.1 \times 10^{-3} \text{ S cm}^{-1}$.¹⁸ Several phosphoric acid and azole doped COFs were also prepared and showed high proton conductivity.¹¹⁻¹³ However, most of COFs required the loading of proton carriers to achieve high proton conductivity. Proton conductivity originates from the external contribution of proton carriers. Under high temperature, the proton carriers are easy to leak, thus the proton conductivity would be reduced. Therefore, it is highly desirable to develop intrinsic proton conducting COFs without loading proton carriers to achieve stable proton conductivity. In this research, we anchored sulfonic acid groups on COF's channel walls for proton conduction via a post-synthetic modification, which is a reliable method in COF's field.¹⁹⁻²¹ The intrinsic proton conductivity of sulfonated 2D COF was investigated.

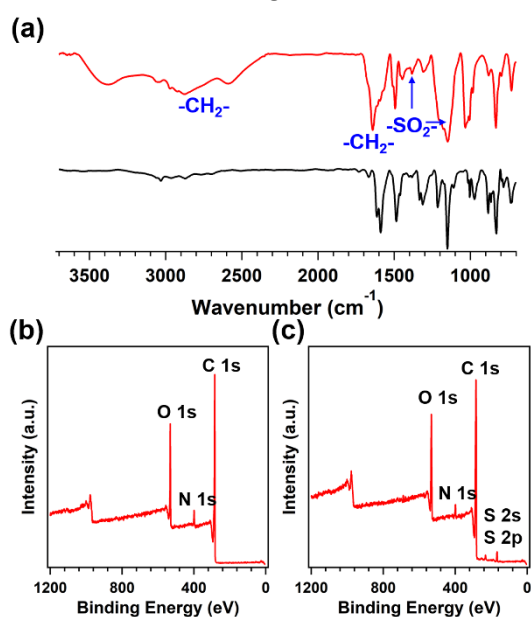


Fig. 1 (a) FT-IR spectra of PyTTA-DHTA-COF (black curve) and PyTTA-DHTA-COF-SO₃H (red). Full XPS scan survey of (b) PyTTA-DHTA-COF and (c) PyTTA-DHTA-COF-SO₃H.

PyTTA-DHTA-COF was synthesized by condensation of 4,4',4'',4'''-(pyrene-1,3,6,8-tetrayl)tetraaniline and 2,5-dihydroxyterephthalaldehyde through Schiff base reaction under solvothermal conditions (Scheme 1). The PyTTA-DHTA-COF kept excellent crystallinity under 1 M NaOH at room temperature (Fig. S1). PyTTA-DHTA-COF-SO₃H that decorated sulfonic acid groups was prepared by reaction with 1,3-propane sulfone under base conditions (Scheme 1). Comparing the red powder of original COF, PyTTA-DHTA-COF-SO₃H showed black powder. Firstly, Fourier transforms infrared spectroscopy (FT-IR) measurements were performed for the as-prepared COFs (Fig. 1a). The characteristic C=N stretching vibration at around 1616 cm^{-1} confirmed the imine bond of COFs was found. After modification, the signal of O=S=O symmetric and asymmetric stretching modes of PyTTA-DHTA-COF-SO₃H was observed at 1178 and 1387 cm^{-1} , respectively. Additionally, a new strong peak for PyTTA-DHTA-COF-SO₃H was observed at 1641 cm^{-1} and several peaks appeared at around 2800 to 3000 cm^{-1} ,

attributing to the -CH₂- stretching vibration of ethylene groups. The X-ray photoelectron spectroscopy (XPS) analysis was performed for PyTTA-DHTA-COF, the C 1s, O 1s, and N 1s signals were clearly observed in the full XPS scan survey (Fig. 1b). The signals for sulfur have been found in PyTTA-DHTA-COF-SO₃H (Fig. 1c). The binding energies of the S 2p_{3/2} and S 2p_{1/2} appeared at 168.6 and 169.1 eV , respectively (Fig. S2). Field emission scanning electron microscopy (FE SEM) images were implemented to investigate the morphology of COFs (Fig. S3). The morphology is no obvious difference between two COFs and this indicated the morphology remained after the sulfonation process. We observed the elemental mapping by energy dispersive spectroscopy (EDS) analysis for COF (Fig. S4). Interestingly, the EDX mapping indicated that the sulfur element is evenly dispersed in the skeleton of sulfonated COF (Fig. S4b). PyTTA-DHTA-COF-SO₃H exhibited moderate sulfur acid group amount of 19.5 wt\% , which was confirmed through elemental analysis (Table S1).

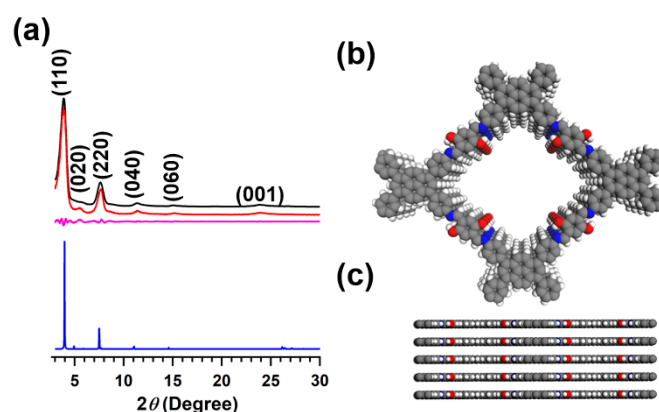


Fig. 2 (a) PXRD patterns of the PyTTA-DHTA-COF (experimentally observed pattern: red; Pawley refinement: black; their difference: pink; AA stacking: blue). (b) Top and (c) side views of the crystal structure of PyTTA-DHTA-COF derived using the AA stacking model.

The crystalline nature of COF was determined by powder X-ray diffraction (PXRD) measurement. The PXRD pattern of PyTTA-DHTA-COF displayed obvious diffraction peaks at two theta of 3.70 , 5.30 , 7.31 , 11.29 , 15.17 and 23.69° , which were assignable to (110), (020), (220), (040), (060), and (001) facets, respectively (Fig. 2). The Pawley refined pattern (Fig. 2a, black) confirmed the diffraction peak assignments of the observed diffraction peaks (Fig. 2a, red). From XRD patterns, it is matched well with AA-mode. Simulations using the P1 space group with $a = 32.3826 \text{ \AA}$, $b = 39.3389 \text{ \AA}$, $c = 3.6909 \text{ \AA}$ and $\alpha = \beta = 90^\circ$, $\gamma = 120^\circ$ gave a PXRD pattern that was in good agreement with the experimentally observed pattern. The staggered AA mode (blue) primarily meted the experimental results with Rwp of 5.65% and Rp of 3.85% . PyTTA-DHTA-COF-SO₃H also remained the crystal structure after post modification and showed broad peaks in comparison with original COF (Fig. S5).

We inspected the porosity of COFs through nitrogen sorption measurements at 77 K (Fig. 3). PyTTA-DHTA-COF has the highest Brunauer-Emmett-Teller (BET) surface area of $2013 \text{ m}^2 \text{ g}^{-1}$ with a pore size of 2.1 nm , which is adjacent to the theoretical result by AA stacking mode of 2.1 nm . This result proved the high

regular 1D channel of PyTTA-DHTA-COF. After the post-modification process, a lower BET surface area of $493 \text{ m}^2 \text{ g}^{-1}$ for PyTTA-DHTA-COF-SO₃H was obtained. PyTTA-DHTA-COF-SO₃H also decreased the pore volume from $1.91 \text{ cm}^3 \text{ g}^{-1}$ (PyTTA-DHTA-COF) to $0.75 \text{ cm}^3 \text{ g}^{-1}$. Pore size was also decreased from 2.1 nm to 1.7 nm due to the pore block by the post-modification process. For a humidity-mediated proton-transport system, it promotes and strengthens proton-exchange/transport efficiency owing to extended hydrogen-bonded frameworks and water molecules. Therefore, the water vapor sorption isotherm of sulfonated COF was measured at 298 K (Fig. S6). PyTTA-DHTA-COF-SO₃H showed a high water uptake of 22.4 mmol g^{-1} , which is comparable to those of reported COFs.²²⁻²⁵

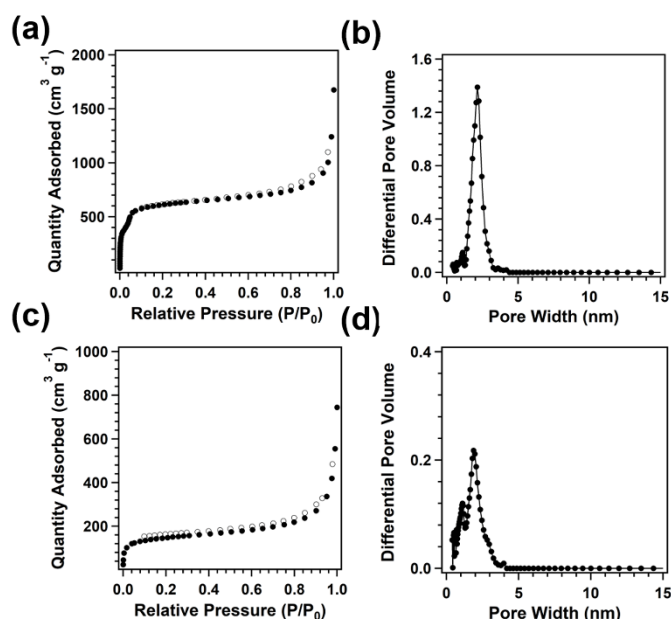


Fig. 3 Nitrogen sorption isotherms of (a) PyTTA-DHTA-COF and (c) PyTTA-DHTA-COF-SO₃H measured at 77 K (●: adsorption, ○: desorption). Pore size distribution profiles of (b) PyTTA-DHTA-COF and (d) PyTTA-DHTA-COF-SO₃H.

PyTTA-DHTA-COF-SO₃H exhibited good porosity, remarkable water uptakes, and plenty of sulfonic acid units, which triggered us to measure the water-mediated proton conductivity. With the increasing humidity, the proton conductivities of PyTTA-DHTA-COF-SO₃H have been improved of 1.0×10^{-6} , 3.2×10^{-5} , 1.4×10^{-4} and $4.9 \times 10^{-4} \text{ S cm}^{-1}$, respectively, under 43%, 53%, 75%, and 85% humidity (Fig. S7). This indicates the crucial role of humidity in the proton conductive process. The proton conductivity dependence on temperature was investigated by testing the materials from 25 to 70 °C under 100% RH (Figs. 4a and S8). PyTTA-DHTA-COF-SO₃H showed the proton conductivities of $3.0 \times 10^{-3} \text{ S cm}^{-1}$ at 25 °C and 100% RH, which is much higher than that of PyTTA-DHTA-COF ($9.5 \times 10^{-5} \text{ S cm}^{-1}$, Figs. 4a and S8) and PyTTA-TA_{0.5}-DHTA_{0.5}-COF-SO₃H_{0.5} under this condition ($4.1 \times 10^{-4} \text{ S cm}^{-1}$, Fig. S9). This indicates that increasing the sulfonic acid groups of PyTTA-DHTA-COF can greatly enhance proton conductivity. We also investigated the temperature dependence on proton conductivity for COFs from 25 to 70 °C under 100% RH. With the increment of temperature, the proton-conducting values of PyTTA-DHTA-COF-SO₃H were

improved (Figs. 4a and S8). PyTTA-DHTA-COF-SO₃H showed the proton conductivities of 6.2×10^{-3} , 1.1×10^{-2} , and $1.6 \times 10^{-2} \text{ S cm}^{-1}$ at 40, 50 and 60 °C, respectively. When increasing the temperature to 70 °C, the conductivity value was as high as $2.0 \times 10^{-2} \text{ S cm}^{-1}$, which ascribes uniform 1D channel affords the way to improve proton transport. This result is comparable to well-performed materials with sulfonic acid groups such as poly(flourenyl ether ketone) ($5.4 \times 10^{-3} \text{ S cm}^{-1}$, 80 °C, water),²⁶ and sulfonated poly(aryl ether) ($1.0 \times 10^{-2} \text{ S cm}^{-1}$, 80 °C, water).²⁷ The time-dependent proton conduction of PyTTA-DHTA-COF-SO₃H was measured and the proton conductivity didn't show any change after 8 h (Fig. S10).

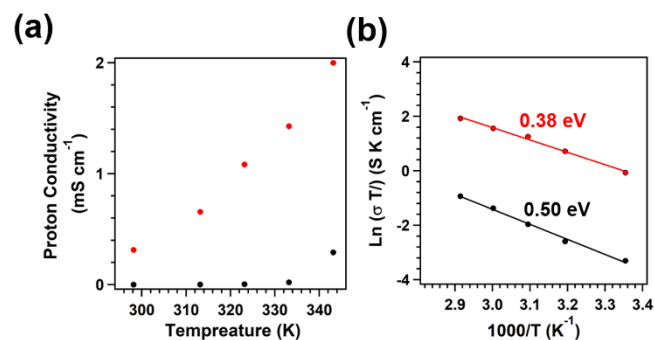


Fig. 4 Proton conductivity of (a) PyTTA-DHTA-COF (black) and PyTTA-DHTA-COF-SO₃H (red) at different temperature and 100% RH. Arrhenius plots for (b) PyTTA-DHTA-COF (black) and PyTTA-DHTA-COF-SO₃H (red).

From linear least-squares fits of the slopes of Arrhenius plots at different temperatures, we calculated the activation energy (EA) of proton-conducting COFs (Fig. 4b). A higher activation energy was determined to be 0.50 eV for PyTTA-DHTA-COF. On the contrary, the PyTTA-DHTA-COF-SO₃H exhibited a lower activation energy of 0.38 eV. These results indicated Grotthuss proton-transport mechanism is shown in the sulfonated COF system. Owing to extended hydrogen-bonding frameworks towards water molecules, a hooping pathway affords a transportation way of the proton and improved the proton-transfer efficiency.

In short, we report the immobilization of flexible sulfonic acid groups on the channel walls of PyTTA-DHTA-COF via a simple post-synthetic modification strategy. The sulfonated COF showed intrinsic proton conductivity up to 10^{-3} at 25 °C and 100% RH, and high conductivity up to $10^{-2} \text{ S cm}^{-1}$ under at 70 °C and 100% RH without introduction of any acid, imidazole or triazole derivatives. This research evolves a new way to design high proton-conductive COFs.

Author Contributions

Y. Zhang and C. Li contributed equally. Y. Zhang, C. Li, Z. Liu, Y. Yao, Md. M. Hasan, Q. Liu, H. Li, J. Wan and Z. Li conducted experiments and collected data collection. Y. Zhang, H. Li, Y. Nagao and Z. Li wrote the manuscript and discussed the results with all authors.

Conflicts of interest

There are no conflicts to declare.

Acknowledgements

Y. Z. appreciated the support by National Natural Science Foundation of China (grant no. 21805110) and the projects of Jilin Province Department of Education (JJKH20210441KJ). H. L. appreciate the support National Natural Science Foundation of China (grant no. 22002162). Y. N. appreciated the support by JSPS KAKENHI grant numbers JP21H00020 and JP21H01997 and The Murata Science Foundation. J. Wan appreciated support from The National Natural Science Foundation of China (No. 51902195)

References

- 1 T. Higashihara, K. Matsumoto and M. Ueda, *Polymer*, 2009, **50**, 5341–5357.
- 2 Y. Nagao, *Langmuir*, 2017, **33**, 12547–12558.
- 3 Y. Nagao, *Sci. Tech. Adv. Mater.*, 2020, **21**, 79–91.
- 4 (a) T. Yamada, K. Otsubo, R. Makiura and H. Kitagawa, *Chem. Soc. Rev.*, 2013, **42**, 6655–6669. (b) P. Jhariat, P. Kumari and T. Panda, *CrystEngComm*, 2020, **22**, 6425–6443.
- 5 (a) Z. Li, Y. Yao, D. Wang, M. M. Hasana, A. Suwansoontorna, H. Li, G. Du, Z. Liu and Y. Nagao, *Mater. Chem. Front.*, 2020, **4**, 2339–2345; (b) Z. Li, Z. Liu, H. Li, Md. M. Hasan, A. Suwansoontorn, G. Du, D. Wang, Y. Zhang and Y. Nagao, *ACS Appl. Polym. Mater.*, 2020, **2**, 3267–3273.
- 6 (a) Y. Li, W. Chen, G. Xing, D. Jiang and L. Chen, *Chem. Soc. Rev.*, 2020, **49**, 2852–2868; (b) H. Li, J. Liu, M. Wang, X. Ren, C. Li, Y. Ren and Q. Yang, *Sol. RRL*, 2021, **5**, 2000641; (c) C. Li, Y. Ma, H. Liu, L. Tao, Y. Ren, X. Chen, H. Li and Q. Yang, *Chin. J. Catal.*, 2020, **41**, 1288–1297; (d) H. Li, H. Liu, C. Li, J. Liu, J. Liu and Q. Yang, *J. Mater. Chem. A*, 2020, **8**, 18745–18754.
- 7 (a) Y. Zhi, Z. Wang, H. Zhang and Q. Zhang, *Small*, 2020, **16**, 2001070; (b) S. Xu and Q. Zhang, *Mater. Today Energy*, 2021, **20**, 100635; (c) J. Yang, F. Kang, X. Wang and Q. Zhang, *Mater. Horiz.*, 2021, DOI: 10.1039/D1MH00809A; (d) C.-J. Yao, Z. Wu, J. Xie, F. Yu, W. Guo, Z. J. Xu, D.-S. Li, S. Zhang and Q. Zhang, *ChemSusChem*, 2020, **13**, 2457–2463; (e) P. She, Y. Qin, X. Wang and Q. Zhang, *Adv. Mater.*, 2021, **33**, 2101175.
- 8 (a) B. Dong, L. Wang, S. Zhao, R. Ge, X. Song, Y. Wang and Y. Gao, *Chem. Commun.*, 2016, **52**, 7082–7085; (b) Q. Yan, H. Xu, X. Jing, H. Hu, S. Wang, C. Zeng and Y. Gao, *RSC Adv.*, 2020, **10**, 17396–17403; (c) L. Zhai, S. Sun, P. Chen, Y. Zhang, Q. Sun, Q. Xu, Y. Wu, R. Nie, Z. Li, L. Mi, *Mater. Chem. Front.*, 2021, **5**, 5463–5470.
- 9 (a) Z. Li, Y. Zhang, H. Xia, Y. Mu and X. Liu, *Chem. Commun.*, 2016, **52**, 6613–6616; (b) Z. Li, K. Geng, T. He, K. T. Tan, N. Huang, Q. Jiang, Y. Nagao and D. Jiang, *Angew. Chem. Int. Ed.*, 2021, **60**, 2–11; (c) D.-M. Li, S.-Y. Zhang, J.-Y. Wan, W.-Q. Zhang, Y.-L. Yan, X.-H. Tang, S.-R. Zheng, S.-L. Cai and W.-G. Zhang, *CrystEngComm*, 2021, **23**, 3594–3601.
- 10 H. Xu, J. Gao and D. Jiang, *Nat. Chem.*, 2015, **7**, 905–912.
- 11 Y. Peng, G. Xu, Z. Hu, Y. Cheng, C. Chi, D. Yuan, H. Cheng and D. Zhao, *ACS Appl. Mater. Interfaces*, 2016, **28**, 18505–18512.
- 12 S. Chandra, T. Kundu, K. Dey, M. Addicoat, T. Heine and R. Banerjee, *Chem. Mater.*, 2016, **28**, 1489–1494.
- 13 D. B. Shinde, H. B. Aiyappa, M. Bhadra, B. P. Biswal, P. Wadge, S. Kandambeth, B. Garai, T. Kundu, S. Kurungot and R. Banerjee, *J. Mater. Chem. A*, 2016, **4**, 2682–2690.
- 14 X. Wu, Y. Hong, B. Xu, Y. Nishiyama, W. Jiang, J. Zhu, G. Zhang, S. Kitagawa and S. Horike, *J. Am. Chem. Soc.*, 2020, **142**, 14357–14364.
- 15 S. Chen, Y. Wu, Y. Zhang, W. Zhang, Y. Fu, W. Huang, T. Yan and H. Ma, *J. Mater. Chem. A*, 2020, **8**, 13702–13709.
- 16 Z. Li, Z. Liu, Z. Li, T. Wang, F. Zhao, X. Ding, W. Feng and B. H. Han, *Adv. Funct. Mater.*, 2020, **30**, 1909267.
- 17 Z. Yang, P. Chen, W. Hao, Z. Xie, Y. Feng, G. Xing and L. Chen., *Chem. Eur. J.*, 2021, **27**, 3817–3822.
- 18 H. Xu, S. Tao and D. Jiang, *Nat. Mater.*, 2016, **15**, 722–726.
- 19 R. A. Maia, B. Louis and S. A. Baudron, *CrystEngComm*, 2021, **23**, 5016–5032.
- 20 J. Segura, S. Royuela and M. M. Ramos, *Chem. Soc. Rev.*, 2019, **48**, 3903–3945.
- 21 H. Ding, A. Mal and C. Wang, *Mater. Chem. Front.*, 2020, **4**, 113–127.
- 22 S. Royuela, E. García-Garrido, M. M. Arroyo, M. J. Mancheño, M. M. Ramos, D. González-Rodríguez, Á. Somoza, F. Zamora and J. L. Segura, *Chem. Commun.*, 2018, **54**, 8729–8732.
- 23 B. P. Biswal, S. Kandambeth, S. Chandra, D. B. Shinde, S. Bera, S. Karak, B. Garai, U. K. Kharul and R. Banerjee, *J. Mater. Chem. A*, 2015, **3**, 23664–23669.
- 24 S. Karak, S. Kandambeth, B. P. Biswal, H. S. Sasmal, S. Kumar, P. Pachfule and R. Banerjee, *J. Am. Chem. Soc.*, 2017, **139**, 1856–1862.
- 25 L. GarzIn-Tovar, J. Perez-Carvajal, A. Yazdi, J. Hernandez-Munoz, P. Tarazona, I. Imaz, F. Zamora and D. MasPOCH, *Angew. Chem. Int. Ed.*, 2019, **58**, 9512–9516.
- 26 T. Suda, K. Yamazaki and H. Kawakami, *J. Power Sources*, 2010, **195**, 4641–4646.
- 27 S. Tian, D. Shu, S. Wang, M. Xiao and Y. Meng, *Fuel Cells* 2007, **7**, 232–237.